

A Uniform and Pressure-Robust Enriched Galerkin Method for the Brinkman Equations

Seulip Lee¹ • Lin Mu¹

Received: 10 July 2023 / Revised: 29 February 2024 / Accepted: 3 March 2024 /

Published online: 28 March 2024

© The Author(s), under exclusive licence to Springer Science+Business Media, LLC, part of Springer Nature 2024

Abstract

This paper presents a pressure-robust enriched Galerkin (EG) method for the Brinkman equations with minimal degrees of freedom based on EG velocity and pressure spaces. The velocity space consists of linear Lagrange polynomials enriched by a discontinuous, piecewise linear, and mean-zero vector function per element, while piecewise constant functions approximate the pressure. Since the Brinkman equations can be seen as a combination of the Stokes and Darcy equations, different conformities of finite element spaces are required depending on viscous parameters, making it challenging to develop a robust numerical solver uniformly performing for all viscous parameters. Therefore, we propose a pressure-robust method by utilizing a velocity reconstruction operator and replacing EG velocity functions with a reconstructed velocity. The robust method leads to error estimates independent of a pressure term and shows uniform performance for all viscous parameters, preserving minimal degrees of freedom. We prove well-posedness and error estimates for the robust EG method while comparing it with a standard EG method requiring an impractical mesh condition. We finally confirm theoretical results through numerical experiments with two- and three-dimensional examples and compare the methods' performance to support the need for our robust method.

Keywords Enriched Galerkin finite element methods · Brinkman equations · Pressure-robust · Velocity reconstruction · Uniform performance

Mathematics Subject Classification 65N15 · 65N30 · 76D07

Lin Mu's work was supported in part by the U.S. National Science Foundation grant DMS-2309557.

✓ Seulip Lee seulip.lee@uga.eduLin Mu

linmu@uga.edu

Department of Mathematics, University of Georgia, Athens, GA 30602, USA



1 Introduction

We consider the stationary Brinkman equations in a bounded domain $\Omega \subset \mathbb{R}^d$ for d=2,3with simply connected Lipschitz boundary $\partial \Omega$. The Brinkman equations describe fluid flow in porous media characterized by interconnected pores that allow for the flow of fluids, considering both the viscous forces within the fluid and the resistance from the porous media. The Brinkman equations provide a mathematical framework for studying and modeling complex phenomena such as groundwater flow, multiphase flow in oil reservoirs, blood flow in biological tissues, and pollutant transport in porous media. In this paper, for simplicity, we consider the scaled Brinkman equations for fluid velocity $\mathbf{u}:\Omega\to\mathbb{R}^d$ and pressure $p:\Omega\to\mathbb{R},$

$$-\nu \Delta \mathbf{u} + \mathbf{u} + \nabla p = \mathbf{f} \quad \text{in } \Omega, \tag{1.1a}$$

$$\nabla \cdot \mathbf{u} = 0 \quad \text{in } \Omega, \tag{1.1b}$$

$$\mathbf{u} = 0 \quad \text{on } \partial\Omega, \tag{1.1c}$$

where $\nu \in [0, 1]$ is a viscous parameter. Mathematically, the Brinkman equations can be seen as a combination of the Stokes and Darcy equations. When $\nu \to 1$, the Brinkman equations approach a Stokes regime affected by the viscous forces, so standard mixed formulations require the H^1 -conformity for velocity. On the other hand, since the Darcy model becomes more prominent as $\nu \to 0$, finite-dimensional spaces for velocity are forced to satisfy the H(div)-conformity. This compatibility in velocity spaces makes it challenging to construct robust numerical solvers for the Brinkman equations in both the Stokes and Darcy regimes. The numerical tests in [10, 18] show that standard mixed methods with well-known inf-sup stable Stokes elements, such as MINI and Taylor-Hood elements, produce suboptimal orders of convergence in the Darcy regime. Moreover, with piecewise constant approximations for pressure, the standard methods' velocity errors do not converge in the Darcy regime, while mesh size decreases. On the other hand, Darcy elements such as Raviart-Thomas and Brezzi-Douglas-Marini do not work for the Stokes regime because they do not satisfy the H^1 -conformity. Therefore, the development of robust numerical solvers for the Brinkman equations has had considerable attention.

There have been three major categories in developing robust numerical methods for the Brinkman equations. The first category considers Stokes/Darcy elements and adds stabilization (or penalty) terms or degrees of freedom to impose normal/tangential continuity, respectively. This approach allows Stokes elements to cover the Darcy regime [3, 21] or H(div)-conforming finite elements to be extended to the Stokes regime [14–16, 21]. Also, the stabilized method in [2] coarsens a pressure space and applies a stabilization term on pressure, while the robust method in [18] uses an enlarged velocity space. The second approach is to introduce another meaningful unknown and define its suitable formulation and finitedimensional space, such as velocity gradient [7, 9, 11, 24], vorticity [1, 5, 20], pseudostress [8], and Lagrange multipliers at elements' boundaries [13]. The third direction is the development of a velocity reconstruction operator, first introduced in [17], mapping Stokes elements into an H(div)-conforming space. In a discrete problem for the Brinkman equations, reconstructed velocity functions replace Stokes elements in the Darcy term and the test function on the right-hand side. This idea has been adopted for a uniformly robust weak Galerkin method for the Brinkman equations [19], which inspires our work because of its simplicity in modification.

The enriched Galerkin (EG) velocity and pressure spaces have been proposed by [22, 23] for solving the Stokes equations with minimal degrees of freedom, keeping local mass



conservation. The velocity space consists of linear Lagrange polynomials enriched by a discontinuous, piecewise linear, and mean-zero vector function per element, while piecewise constant functions approximate the pressure. More precisely, a velocity function $\mathbf{v} = \mathbf{v}^C + \mathbf{v}^D$ consists of a continuous linear Lagrange polynomial \mathbf{v}^C and a discontinuous piecewise linear enrichment function \mathbf{v}^D , so interior penalty discontinuous Galerkin (IPDG) formulations are adopted to remedy the discontinuity of \mathbf{v}^D . These velocity and pressure spaces satisfy the inf-sup condition for the Stokes equations, so they are stable Stokes elements.

Our research focuses on developing a robust numerical method for the Brinkman equations using the EG velocity and pressure spaces with minimal degrees of freedom. Since the EG spaces are stable Stokes elements, simply adding the Darcy term $(\mathbf{u}, \mathbf{v})_{\Omega}$ to the Stokes discrete problem in [22] only works for the Brinkman equations in the Stokes regime. However, such a standard approach fails to produce accurate velocity solutions in the Darcy regime despite decreasing mesh size before resolving a mesh size condition, $h < \sqrt{\nu}$, impractical in the Darcy regime. Hence, to develop a robust EG method, we employ the velocity reconstruction operator [12] (inspired by [17]) to map the EG velocity to the first-order Brezzi-Douglas-Marini space, whose consequent action is preserving the continuous component \mathbf{v}^C and mapping only the discontinuous component \mathbf{v}^D to the lowest-order Raviart-Thomas space. Compared to the Stokes solver in [12] modifying only the right-hand side, we replace the EG velocities in the Darcy term and on the right-hand side with the reconstructed linear H(div)conforming velocity. Therefore, with this simple modification, our resulting EG method yields pressure-robust error estimates and shows uniform performance from the Stokes to Darcy regime (including $\nu = 0$) without any restriction in mesh size. Through two- and three-dimensional examples, we compare the numerical performance of the standard and robust EG methods with the viscous parameter $\nu \in [0, 1]$ and mesh size h, emphasizing the robust EG method's uniform performance in solving the Brinkman equations. Compared to the existing numerical solvers for Brinkman-Darcy coupled problems with sharp interface, our method considers one governing equation in the whole domain using variable viscosity or permeability without requiring appropriate numerical schemes in different subdomains. The challenge in the sharp interface setting may need advanced finite element functions/schemes and different analysis techniques in error estimates. Our robust method can overcome such difficulties by implementing the Brinkman equations uniformly.

The remaining sections of this paper are structured as follows: Some important notations and definitions are introduced in Sect. 2. In Sect. 3, we present the standard and robust EG methods for the Brinkman equations, recalling the EG velocity and pressure spaces [22] and the velocity reconstruction operator [12]. We prove the well-posedness and error estimates of the EG methods in Sect. 4, verifying the uniform performance of the robust method from the Stokes to Darcy regimes. Section 5 validates our theoretical results through numerical experiments in two and three dimensions. Finally, we summarize our contribution in this paper and discuss related future research in Sect. 6.

2 Preliminaries

In this section, we introduce some notations and definitions used in this paper. For a bounded Lipschitz domain $\mathcal{D} \in \mathbb{R}^d$, where d=2,3, we denote the Sobolev space as $H^s(\mathcal{D})$ for a real number $s \geq 0$. Its norm and seminorm are denoted by $\|\cdot\|_{s,\mathcal{D}}$ and $\|\cdot\|_{s,\mathcal{D}}$, respectively. The space $H^0(\mathcal{D})$ coincides with $L^2(\mathcal{D})$, and the L^2 -inner product is denoted by $(\cdot,\cdot)_{\mathcal{D}}$. When $\mathcal{D}=\Omega$, the subscript \mathcal{D} will be omitted. This notation is generalized to vector- and



tensor-valued Sobolev spaces. The notation $H_0^1(\mathcal{D})$ means the space of $v \in H^1(\mathcal{D})$ such that v=0 on $\partial \mathcal{D}$, and $L_0^2(\mathcal{D})$ means the space of $v\in L^2(\mathcal{D})$ such that $(v,1)_{\mathcal{D}}=0$. The polynomial spaces of degree less than or equal to k are denoted as $P_k(\mathcal{D})$. We also introduce the Hilbert space

$$H(\operatorname{div}, \mathcal{D}) := \{ \mathbf{v} \in [L^2(\mathcal{D})]^d : \operatorname{div} \mathbf{v} \in L^2(\mathcal{D}) \}$$

with the norm

$$\|\mathbf{v}\|_{H(\text{div},\mathcal{D})}^2 := \|\mathbf{v}\|_{0,\mathcal{D}}^2 + \|\text{div }\mathbf{v}\|_{0,\mathcal{D}}^2.$$

For discrete setting, we assume that there exists a shape-regular triangulation \mathcal{T}_h of Ω whose elements $T \in \mathcal{T}_h$ are triangles in two dimensions and tetrahedrons in three dimensions. Also, \mathcal{E}_h denotes the collection of all edges/faces in \mathcal{T}_h , and $\mathcal{E}_h = \mathcal{E}_h^o \cup \mathcal{E}_h^b$, where \mathcal{E}_h^o is the collection of all the interior edges/faces and \mathcal{E}_h^b is that of the boundary edges/faces. For each element $T \in \mathcal{T}_h$, let h_T denote the diameter of T and \mathbf{n}_T denote the outward unit normal vector on ∂T . For each interior edge/face $e \in \mathcal{E}_h^o$ shared by two adjacent elements T^+ and T^- , we let \mathbf{n}_e be the unit normal vector from T^+ to T^- . For each $e \in \mathcal{E}_h^b$, \mathbf{n}_e denotes the outward unit normal vector on $\partial \Omega$. In a triangulation \mathcal{T}_h , the broken Sobolev space is defined as

$$H^s(\mathcal{T}_h) := \{ v \in L^2(\Omega) : v|_T \in H^s(T), \ \forall T \in \mathcal{T}_h \},$$

equipped with the norm

$$\|v\|_{s,\mathcal{T}_h} := \left(\sum_{T \in \mathcal{T}_h} \|v\|_{s,T}^2\right)^{1/2}.$$

When s = 0, the L^2 -inner product on \mathcal{T}_h is denoted by $(\cdot, \cdot)_{\mathcal{T}_h}$. Also, the L^2 -inner product on \mathcal{E}_h is denoted as $\langle \cdot, \cdot \rangle_{\mathcal{E}_h}$, and the L^2 -norm on \mathcal{E}_h is defined as

$$\|v\|_{0,\mathcal{E}_h} := \left(\sum_{e \in \mathcal{E}_h} \|v\|_{0,e}^2\right)^{1/2}.$$

The piecewise polynomial space corresponding to the broken Sobolev space is defined as

$$P_k(\mathcal{T}_h) = \{ v \in L^2(\Omega) : v|_T \in P_k(T), \ \forall T \in \mathcal{T}_h \}.$$

In addition, the jump and average of v on $e \in \mathcal{E}_h$ are defined as

$$[v] := \begin{cases} v^+ - v^- \text{ on } e \in \mathcal{E}_h^o, \\ v \text{ on } e \in \mathcal{E}_h^b, \end{cases} \quad \{v\} := \begin{cases} (v^+ + v^-)/2 \text{ on } e \in \mathcal{E}_h^o, \\ v \text{ on } e \in \mathcal{E}_h^b, \end{cases}$$

where v^{\pm} is the trace of $v|_{T^{\pm}}$ on $e \in \partial T^{+} \cap \partial T^{-}$. These definitions are extended to vector- and tensor-valued functions. We finally introduce the trace inequality that holds for any function $v \in H^1(T)$,

$$||v||_{0,e}^2 \le C \left(h_T^{-1} ||v||_{0,T}^2 + h_T ||\nabla v||_{0,T}^2 \right). \tag{2.1}$$

3 Enriched Galerkin Methods for the Brinkman Equations

We first introduce the enriched Galerkin (EG) finite-dimensional velocity and pressure spaces [22]. The space of continuous components for velocity is

$$\mathbf{C}_h = {\{\mathbf{v}^C \in [H_0^1(\Omega)]^d : \mathbf{v}^C|_T \in [P_1(T)]^d, \ \forall T \in \mathcal{T}_h\}}.$$



The space of discontinuous components for velocity is defined as

$$\mathbf{D}_h = \{ \mathbf{v}^D \in L^2(\Omega) : \mathbf{v}^D |_T = c(\mathbf{x} - \mathbf{x}_T), \ c \in \mathbb{R}, \ \forall T \in \mathcal{T}_h \},$$

where \mathbf{x}_T is the barycenter of $T \in \mathcal{T}_h$. Thus, the EG finite-dimensional velocity space is defined as

$$\mathbf{V}_h := \mathbf{C}_h \oplus \mathbf{D}_h$$
.

We note that any function $\mathbf{v} \in \mathbf{V}_h$ consists of unique continuous and discontinuous components, $\mathbf{v} = \mathbf{v}^C + \mathbf{v}^D$ for $\mathbf{v}^C \in \mathbf{C}_h$ and $\mathbf{v}^D \in \mathbf{D}_h$. At the same time, the EG pressure space is

$$Q_h := \{ q \in L_0^2(\Omega) : q|_T \in P_0(T), \ \forall T \in \mathcal{T}_h \}.$$

Therefore, we formulate a standard EG method for the Brinkman equations with the pair of the EG spaces $V_h \times Q_h$ by adding the Darcy term to the Stokes formulation [22].

Algorithm 1 Standard enriched Galerkin (ST-EG) method

Find $(\mathbf{u}_h, p_h) \in \mathbf{V}_h \times Q_h$ such that

$$\nu \mathbf{a}(\mathbf{u}_h, \mathbf{v}) + \mathbf{c}(\mathbf{u}_h, \mathbf{v}) - \mathbf{b}(\mathbf{v}, p_h) = (\mathbf{f}, \mathbf{v}) \qquad \forall \mathbf{v} \in \mathbf{V}_h, \tag{3.1a}$$

$$\mathbf{b}(\mathbf{u}_h, q) = 0 \qquad \forall q \in Q_h, \tag{3.1b}$$

where

$$\begin{aligned} \mathbf{a}(\mathbf{v}, \mathbf{w}) &:= (\nabla \mathbf{v}, \nabla \mathbf{w})_{\mathcal{T}_h} - \langle \{\nabla \mathbf{v}\} \mathbf{n}_e, [\mathbf{w}] \rangle_{\mathcal{E}_h} \\ &- \langle \{\nabla \mathbf{w}\} \mathbf{n}_e, [\mathbf{v}] \rangle_{\mathcal{E}_h} + \rho \langle h_e^{-1} [\mathbf{v}], [\mathbf{w}] \rangle_{\mathcal{E}_h}, \end{aligned} \tag{3.2a}$$

$$\mathbf{c}(\mathbf{v}, \mathbf{w}) := (\mathbf{v}, \mathbf{w})_{\mathcal{T}_h},\tag{3.2b}$$

$$\mathbf{b}(\mathbf{w}, q) := (\nabla \cdot \mathbf{w}, q)_{\mathcal{T}_h} - \langle [\mathbf{w}] \cdot \mathbf{n}_e, \{q\} \rangle_{\mathcal{E}_h}. \tag{3.2c}$$

In this case, $\rho > 0$ is a penalty parameter, and $h_e = |e|^{1/(d-1)}$, where |e| is the length/area of the edge/face $e \in \mathcal{E}_h$.

Remark 1 Since the enriched functions in \mathbf{D}_h contain discontinuity, Algorithm 1 employs interior penalty discontinuous Galerkin (IPDG) formulations for well-posedness. The symmetric, non-symmetric, and incomplete IPDG methods can be applied under suitable assumptions of ρ , as discussed in [21]. For simplicity, we only consider the symmetric IPDG formulation because we can easily extend the symmetric method's results to the other IPDG methods. On the other hand, for the cases with small $\nu \ (\ll 1)$, the ST-EG method fails to produce stable and accurate velocity solutions unless mesh size satisfies the impractical condition $h < \sqrt{\nu}$. For this reason, we will improve it by imposing a velocity reconstruction operator.

We develop a pressure-robust EG method for the Brinkman equations with any value of $\nu \in [0, 1]$. First, the velocity reconstruction operator [12] is defined as $\mathcal{R}: \mathbf{V}_h \to \mathcal{B}DM_1(\mathcal{T}_h) \subset H(\text{div}, \Omega)$ such that

$$\int_{e} (\mathcal{R}\mathbf{v}) \cdot \mathbf{n}_{e} p_{1} ds = \int_{e} \{\mathbf{v}\} \cdot \mathbf{n}_{e} p_{1} ds, \qquad \forall p_{1} \in P_{1}(e), \ \forall e \in \mathcal{E}_{h}^{o}, \qquad (3.3a)$$



$$\int_{e} (\mathcal{R}\mathbf{v}) \cdot \mathbf{n}_{e} p_{1} ds = 0, \qquad \forall p_{1} \in P_{1}(e), \ \forall e \in \mathcal{E}_{h}^{b}, \qquad (3.3b)$$

where $\mathcal{B}DM_1(\mathcal{T}_h)$ is the Brezzi-Douglas-Marini space of index 1 on \mathcal{T}_h . Then, we propose the pressure-robust EG method as follows.

Algorithm 2 Pressure-robust enriched Galerkin (PR-EG) method

Find $(\mathbf{u}_h, p_h) \in \mathbf{V}_h \times Q_h$ such that

$$v\mathbf{a}(\mathbf{u}_h, \mathbf{v}) + \tilde{\mathbf{c}}(\mathbf{u}_h, \mathbf{v}) - \mathbf{b}(\mathbf{v}, p_h) = (\mathbf{f}, \mathcal{R}\mathbf{v}) \qquad \forall \mathbf{v} \in \mathbf{V}_h, \tag{3.4a}$$

$$\mathbf{b}(\mathbf{u}_h, q) = 0 \qquad \forall q \in Q_h, \tag{3.4b}$$

where $\mathbf{a}(\mathbf{v}, \mathbf{w})$ and $\mathbf{b}(\mathbf{v}, \mathbf{w})$ are defined in (3.2a) and (3.2c), respectively, and

$$\tilde{\mathbf{c}}(\mathbf{v}, \mathbf{w}) := (\mathcal{R}\mathbf{v}, \mathcal{R}\mathbf{w})_{\mathcal{T}_b}. \tag{3.5}$$

Remark 2 Using the velocity reconstruction operator \mathcal{R} , we force discrete velocity functions in V_h to be H(div)-conforming. We replace the velocity functions in the Darcy bilinear form $(\mathbf{v}, \mathbf{w})_{\mathcal{T}_h}$ in (3.2b) and on the right-hand side with the reconstructed velocity $\mathcal{R}\mathbf{v}$. Thus, as $\nu \to 0$, the term $(\mathcal{R}\mathbf{v}, \mathcal{R}\mathbf{w})_{\mathcal{T}_h}$ with the H(div)-conforming velocity dominates the PR-EG formulation in Algorithm 2. This modification leads to stable and accurate velocity and pressure solutions with any $\nu \in [0, 1]$, demonstrated by the optimal convergence orders in error analysis in Sect. 4 and numerical experiments in Sect. 5.

4 Well-Posedness and Error Analysis

In this section, we show well-posedness and error estimates for both ST-EG and PR-EG methods, focusing more on the PR-EG method's analysis. The error estimates demonstrate that:

- The PR-EG method's velocity and pressure errors decrease in the optimal order of convergence in both the Stokes and Darcy regimes, so we expect stable and accurate numerical solutions with any $\nu \geq 0$ as h decreases.
- The ST-EG method's errors converge in the first order with h under the condition $h < \sqrt{\nu}$ impractical in the Darcy regime, highlighting the need for the PR-EG method.

We first introduce the discrete H^1 -norm in [22] for all $\mathbf{v} \in [H^1_0(\Omega)]^d$,

$$\|\mathbf{v}\|_{\mathcal{E}}^2 := \|\nabla \mathbf{v}\|_{0,\mathcal{T}_h}^2 + \rho \|h_e^{-1/2}[\mathbf{v}]\|_{0,\mathcal{E}_h}^2,$$

where ρ is a penalty parameter. With this norm, the coercivity and continuity results for the bilinear form $\mathbf{a}(\cdot, \cdot)$ have been proved in [22]: For a sufficiently large penalty parameter ρ , there exist positive constants κ_1 and κ_2 independent of ν and h such that

$$\mathbf{a}(\mathbf{v}, \mathbf{v}) \ge \kappa_1 \|\mathbf{v}\|_{\mathcal{E}}^2 \qquad \forall \mathbf{v} \in \mathbf{V}_h, \tag{4.1}$$

$$|\mathbf{a}(\mathbf{v}, \mathbf{w})| \le \kappa_2 \|\mathbf{v}\|_{\mathcal{E}} \|\mathbf{w}\|_{\mathcal{E}} \qquad \forall \mathbf{v}, \mathbf{w} \in \mathbf{V}_h.$$
 (4.2)

Then, we define an energy norm for Brinkman problems involving the discrete H^1 -norm and L^2 -norm.

$$\|\mathbf{v}\|^2 := \nu \|\mathbf{v}\|_{\mathcal{E}}^2 + \|\mathbf{v}\|_0^2.$$



The following lemma shows an essential norm equivalence between $\| \cdot \|$ and $\| \cdot \|_{\mathcal{E}}$ scaled by ν and h.

Lemma 1 For given v and h, we define a positive constant C_{NE} (Norm Equivalence) as

$$C_{\text{NE}} := C\sqrt{\nu + h^2}$$

where C is a generic positive constant independent of v and h. Then, the following norm equivalence holds: For any $\mathbf{v} \in \mathbf{V}_h$, we have

$$\sqrt{\nu} \|\mathbf{v}\|_{\mathcal{E}} \le \sqrt{\nu + c_1 h^2} \|\mathbf{v}\|_{\mathcal{E}} \le \|\|\mathbf{v}\|\| \le C_{\text{NE}} \|\mathbf{v}\|_{\mathcal{E}},\tag{4.3}$$

for some small $0 < c_1 < 1$. Moreover, the constant C_{NE} is bounded as

$$C_{\text{NE}} < C(\sqrt{\nu} + h) \tag{4.4}$$

for some generic constant C > 0.

Proof We observe each term in the energy norm

$$\|\mathbf{v}\|^2 = \nu \|\mathbf{v}\|_{\mathcal{E}}^2 + \|\mathbf{v}\|_0^2.$$

Since $\mathbf{v}|_T$ is a linear polynomial in the second term, a scaling argument implies

$$\|\mathbf{v}\|_{0} \leq Ch\|\nabla\mathbf{v}\|_{0,\mathcal{T}_{h}} \leq Ch\|\mathbf{v}\|_{\mathcal{E}}.$$

Thus, we obtain

$$\|\|\mathbf{v}\|\|^2 \le C (\nu + h^2) \|\mathbf{v}\|_{\mathcal{E}}^2$$

On the other hand, the inverse and trace inequalities lead to

$$\|\mathbf{v}\|_{\mathcal{E}}^2 \le Ch^{-2}\|\mathbf{v}\|_0^2,$$

where C contains ρ_1 . In this case, we assume C > 1 and set $c_1 := 1/C$, so

$$(\nu + c_1 h^2) \|\mathbf{v}\|_{\mathcal{E}}^2 \le \|\mathbf{v}\|^2.$$

Let us introduce the interpolation operator in [23] $\Pi_h : [H^2(\Omega)]^d \to \mathbf{V}_h$ defined by

$$\Pi_h \mathbf{w} = \Pi_h^C \mathbf{w} + \Pi_h^D \mathbf{w},$$

where $\Pi_h^C \mathbf{w} \in \mathbf{C}_h$ is the nodal value interpolant of \mathbf{w} and $\Pi_h^D \mathbf{w} \in \mathbf{D}_h$ satisfies $(\nabla \cdot \Pi_h^D \mathbf{w}, 1)_T = (\nabla \cdot (\mathbf{w} - \Pi_h^C \mathbf{w}), 1)_T$ for all $T \in \mathcal{T}_h$. The following interpolation error estimates and stability [23] are used throughout our numerical analysis:

$$|\mathbf{w} - \Pi_h \mathbf{w}|_{j,T_h} \le Ch^{m-j} |\mathbf{w}|_m, \qquad 0 \le j \le m \le 2, \quad \forall \mathbf{w} \in [H^2(\Omega)]^d,$$
 (4.5a)

$$\|\mathbf{w} - \Pi_h \mathbf{w}\|_{\mathcal{E}} < Ch\|\mathbf{w}\|_2, \qquad \forall \mathbf{w} \in [H^2(\Omega)]^d, \tag{4.5b}$$

$$\|\Pi_h \mathbf{w}\|_{\mathcal{E}} \le C|\mathbf{w}|_1, \qquad \forall \mathbf{w} \in [H_0^1(\Omega)]^d.$$
 (4.5c)

For the pressure, we introduce the local L^2 -projection $\mathcal{P}_0: H^1(\Omega) \to Q_h$ such that $(q - \mathcal{P}_0q, 1)_T = 0$ for all $T \in \mathcal{T}_h$. Its interpolation error estimate is given as,

$$\|q - \mathcal{P}_0 q\|_0 \le Ch\|q\|_1, \quad \forall q \in H^1(\Omega).$$
 (4.6)



The operator \mathcal{R} defined in (3.3) has the following interpolation error estimate [12]:

$$\|\mathbf{v} - \mathcal{R}\mathbf{v}\|_{0} \le Ch\|h_{e}^{-1/2}[\mathbf{v}]\|_{0,\mathcal{E}_{h}} \le Ch\|\mathbf{v}\|_{\mathcal{E}}, \quad \forall \mathbf{v} \in \mathbf{V}_{h}, \tag{4.7}$$

where C is a positive constant independent of ν and h.

The interpolation error estimate (4.7) allows to have a lower bound of $\| \| \mathbf{v} \| \|$ with another energy norm

$$\|\mathbf{v}\|_{\mathcal{R}}^2 := \nu \|\mathbf{v}\|_{\mathcal{E}}^2 + \|\mathcal{R}\mathbf{v}\|_0^2$$

obtained by replacing $\|\mathbf{v}\|_0$ in $\|\|\mathbf{v}\|\|$ with $\|\mathcal{R}\mathbf{v}\|_0$.

Lemma 2 *For any* $\mathbf{v} \in \mathbf{V}_h$, *it holds*

$$\|\mathbf{v}\|_{\mathcal{R}} \le c^* \|\mathbf{v}\|,\tag{4.8}$$

where c^* is a positive constant independent of v and h.

Proof It follows from (4.7) and Lemma 1 that

$$v \|\mathbf{v}\|_{\mathcal{E}}^{2} + \|\mathcal{R}\mathbf{v}\|_{0}^{2} \leq C \left(v \|\mathbf{v}\|_{\mathcal{E}}^{2} + c_{1}h^{2} \|\mathbf{v}\|_{\mathcal{E}}^{2} + \|\mathbf{v}\|_{0}^{2}\right) \leq C \|\mathbf{v}\|^{2}.$$

4.1 Well-Posedness of the PR-EG Method

We first prove the coercivity and continuity results concerning the energy norm $\|\cdot\|_{\mathcal{R}}$.

Lemma 3 For any \mathbf{v} , $\mathbf{w} \in \mathbf{V}_h$, we have the coercivity and continuity results:

$$\nu \mathbf{a}(\mathbf{v}, \mathbf{v}) + \tilde{\mathbf{c}}(\mathbf{v}, \mathbf{v}) \ge K_1 \|\|\mathbf{v}\|\|_{\mathcal{R}}^2, \tag{4.9}$$

$$|\nu \mathbf{a}(\mathbf{v}, \mathbf{w}) + \tilde{\mathbf{c}}(\mathbf{v}, \mathbf{w})| \le K_2 |||\mathbf{v}|||_{\mathcal{R}} |||\mathbf{w}||_{\mathcal{R}},$$
 (4.10)

where $K_1 = \min(\kappa_1, 1)$ and $K_2 = \max(\kappa_2, 1)$. The constants κ_1 and κ_2 are defined in (4.1) and (4.2), respectively.

Proof If we observe the bilinear forms $\mathbf{a}(\cdot,\cdot)$ and $\tilde{\mathbf{c}}(\cdot,\cdot)$ and use the coercivity (4.1), then we have

$$\nu \mathbf{a}(\mathbf{v}, \mathbf{v}) + \tilde{\mathbf{c}}(\mathbf{v}, \mathbf{v}) \ge \kappa_1 \nu \|\mathbf{v}\|_{\mathcal{E}}^2 + \|\mathcal{R}\mathbf{v}\|_0^2$$

$$\ge \min(\kappa_1, 1) \|\mathbf{v}\|_{\mathcal{R}}^2.$$

Moreover, it follows from the Cauchy–Schwarz inequality and the continuity (4.2) that

$$\begin{aligned} |\nu \mathbf{a}(\mathbf{v}, \mathbf{w}) + \tilde{\mathbf{c}}(\mathbf{v}, \mathbf{w})| &\leq \kappa_2 \nu \|\mathbf{v}\|_{\mathcal{E}} \|\mathbf{w}\|_{\mathcal{E}} + \|\mathcal{R}\mathbf{v}\|_0 \|\mathcal{R}\mathbf{w}\|_0 \\ &\leq \max(\kappa_2, 1) \|\mathbf{v}\|_{\mathcal{R}} \|\mathbf{w}\|_{\mathcal{R}}. \end{aligned}$$

Next, we prove the discrete inf-sup condition for the problem (3.4) in Algorithm 2.

Lemma 4 Assume that the penalty parameter ρ_1 is sufficiently large. Then, there exists a positive constant $C_1 := C_{IS}/(c^*C_{NE})$ such that

$$\inf_{q \in \mathcal{Q}_h} \sup_{\mathbf{v} \in \mathbf{V}_h} \frac{\mathbf{b}(\mathbf{v}, q)}{\|\mathbf{v}\|_{\mathcal{R}} \|q\|_0} \ge C_1, \tag{4.11}$$

where $C_{\rm IS} > 0$ (Inf-Sup), independent of v and h, is the constant for the discrete inf-sup condition in [22]. The constants C_{NE} and c^* are defined in Lemmas 1 and 2, respectively.



Proof We first recall the results of discrete inf-sup condition in [22]: For any $q \in Q_h \subset L_0^2(\Omega)$, there exist a vector $\mathbf{v} \in [H_0^1(\Omega)]^d$ and a constant $C_{\mathrm{IS}} > 0$ independent of h and ν such that

$$C_{\text{IS}} \|q\|_0 \leq \frac{\mathbf{b}(\Pi_h \mathbf{v}, q)}{\|\Pi_h \mathbf{v}\|_{\mathcal{E}}}.$$

Thus, by the upper and lower bounds of $\|\mathbf{v}\|$ in (4.3) and (4.8), we obtain

$$C_{\text{IS}} \|q\|_{0} \le C_{\text{NE}} \frac{\mathbf{b}(\Pi_{h}\mathbf{v}, q)}{\|\|\Pi_{h}\mathbf{v}\|\|} \le c^{*}C_{\text{NE}} \frac{\mathbf{b}(\Pi_{h}\mathbf{v}, q)}{\|\|\Pi_{h}\mathbf{v}\|\|_{\mathcal{R}}}.$$

Therefore, we obtain the well-posedness of the PR-EG method in Algorithm 2.

Theorem 1 There exists a unique solution $(\mathbf{u}_h, p_h) \in \mathbf{V}_h \times Q_h$ to the PR-EG method.

Proof It suffices to show that $\mathbf{u}_h = \mathbf{0}$ and $p_h = 0$ when $\mathbf{f} = \mathbf{0}$ because \mathbf{V}_h and Q_h are finite-dimensional spaces. Choosing $\mathbf{v} = \mathbf{u}_h$ in (3.4a) and $q = p_h$ in (3.4b) and adding the two equations imply $v\mathbf{a}(\mathbf{u}_h, \mathbf{u}_h) + \tilde{\mathbf{c}}(\mathbf{u}_h, \mathbf{u}_h) = 0$. Hence, $\|\mathbf{u}_h\|_{\mathcal{R}} = 0$ by (4.9), so $\mathbf{u}_h = \mathbf{0}$. If $\mathbf{u}_h = \mathbf{0}$ in (3.4), then $\mathbf{b}(\mathbf{v}, p_h) = 0$ for all $\mathbf{v} \in \mathbf{V}_h$. Therefore, the inf-sup condition (4.11) yields $\|p_h\|_0 = 0$, so $p_h = 0$.

Remark 3 Most of the results for the well-posedness of the ST-EG method in Algorithm 1 are similar to those of the PR-EG method. Thus, we omit the details here.

4.2 Error Estimates for the PR-EG Method

Let $(\mathbf{u}, p) \in [H_0^1(\Omega) \cap H^2(\Omega)]^d \times [L_0^2(\Omega) \cap H^1(\Omega)]$ be the solution to (1.1a)–(1.1c). We define the error functions used in the error estimates

$$\mathbf{\chi}_h := \mathbf{u} - \Pi_h \mathbf{u}, \quad \mathbf{e}_h := \Pi_h \mathbf{u} - \mathbf{u}_h, \quad \xi_h := p - \mathcal{P}_0 p, \quad \epsilon_h := \mathcal{P}_0 p - p_h.$$

First, we derive error equations in the following lemma.

Lemma 5 For any $\mathbf{v} \in \mathbf{V}_h$ and $q \in Q_h$, we have

$$\nu \mathbf{a}(\mathbf{e}_h, \mathbf{v}) + \tilde{\mathbf{c}}(\mathbf{e}_h, \mathbf{v}) - \mathbf{b}(\mathbf{v}, \epsilon_h) = l_1(\mathbf{u}, \mathbf{v}) + l_2(\mathbf{u}, \mathbf{v}) + l_3(\mathbf{u}, \mathbf{v}), \tag{4.12a}$$

$$\mathbf{b}(\mathbf{e}_h, q) = -\mathbf{b}(\mathbf{\chi}_h, q), \tag{4.12b}$$

where the supplemental bilinear forms are defined as follows:

$$l_1(\mathbf{u}, \mathbf{v}) := \nu \mathbf{a}(\Pi_h \mathbf{u} - \mathbf{u}, \mathbf{v}),$$

$$l_2(\mathbf{u}, \mathbf{v}) := \nu(\Delta \mathbf{u}, \mathcal{R} \mathbf{v} - \mathbf{v})_{\mathcal{T}_h},$$

$$l_3(\mathbf{u}, \mathbf{v}) := (\mathcal{R} \Pi_h \mathbf{u} - \mathbf{u}, \mathcal{R} \mathbf{v})_{\mathcal{T}_h}.$$

Proof Since $-(\Delta \mathbf{u}, \mathbf{v})_{\mathcal{T}_h} = \mathbf{a}(\mathbf{u}, \mathbf{v})$ for any $\mathbf{v} \in \mathbf{V}_h$ from [22], we have

$$-\nu(\Delta \mathbf{u}, \mathcal{R}\mathbf{v})_{\mathcal{T}_h} = -\nu(\Delta \mathbf{u}, \mathbf{v})_{\mathcal{T}_h} - \nu(\Delta \mathbf{u}, \mathcal{R}\mathbf{v} - \mathbf{v})_{\mathcal{T}_h}$$

$$= \nu \mathbf{a}(\mathbf{u}, \mathbf{v}) - \nu(\Delta \mathbf{u}, \mathcal{R}\mathbf{v} - \mathbf{v})_{\mathcal{T}_h}$$

$$= \nu \mathbf{a}(\Pi_h \mathbf{u}, \mathbf{v}) - \nu \mathbf{a}(\Pi_h \mathbf{u} - \mathbf{u}, \mathbf{v}) - \nu(\Delta \mathbf{u}, \mathcal{R}\mathbf{v} - \mathbf{v})_{\mathcal{T}_h}.$$

By the definition of $\tilde{\mathbf{c}}(\cdot, \cdot)$, we also have

$$(\mathbf{u}, \mathcal{R}\mathbf{v})_{\mathcal{T}_h} = \tilde{\mathbf{c}}(\Pi_h\mathbf{u}, \mathbf{v}) - (\mathcal{R}\Pi_h\mathbf{u} - \mathbf{u}, \mathcal{R}\mathbf{v})_{\mathcal{T}_h}.$$



Since $\mathcal{R}\mathbf{v} \cdot \mathbf{n}_T$ is continuous on ∂T and $\nabla \cdot \mathcal{R}\mathbf{v}$ is constant in T, integration by parts implies

$$(\nabla p, \mathcal{R}\mathbf{v})_{\mathcal{T}_h} = -\mathbf{b}(\mathbf{v}, \mathcal{P}_0 p).$$

Hence, we obtain the following equation from (1.1a),

$$\nu \mathbf{a}(\Pi_h \mathbf{u}, \mathbf{v}) + \tilde{\mathbf{c}}(\Pi_h \mathbf{u}, \mathbf{v}) - \mathbf{b}(\mathbf{v}, \mathcal{P}_0 p) =$$

$$(\mathbf{f}, \mathcal{R} \mathbf{v}) + l_1(\mathbf{u}, \mathbf{v}) + l_2(\mathbf{u}, \mathbf{v}) + l_3(\mathbf{u}, \mathbf{v}).$$

If we compare this equation with (3.4a) in the PR-EG method, we arrive at

$$v\mathbf{a}(\mathbf{e}_h, \mathbf{v}) + \tilde{\mathbf{c}}(\mathbf{e}_h, \mathbf{v}) - \mathbf{b}(\mathbf{v}, \epsilon_h) = l_1(\mathbf{u}, \mathbf{v}) + l_2(\mathbf{u}, \mathbf{v}) + l_3(\mathbf{u}, \mathbf{v}).$$

For the second equation (4.12b), the continuity of **u** and (3.4b) in the PR-EG method lead us to

$$(\nabla \cdot \mathbf{u}, q)_{\mathcal{T}_h} = \mathbf{b}(\mathbf{u}, q) = 0 = \mathbf{b}(\mathbf{u}_h, q).$$

We present estimates for the supplementary bilinear forms defined in Lemma 5.

Lemma 6 Assume that $\mathbf{w} \in [H^2(\Omega)]^d$ and $\mathbf{v} \in \mathbf{V}_h$. Then, we have

$$|l_1(\mathbf{w}, \mathbf{v})| \le C\sqrt{\nu}h\|\mathbf{w}\|_2\|\|\mathbf{v}\|\|_{\mathcal{R}},\tag{4.13a}$$

$$|l_2(\mathbf{w}, \mathbf{v})| \le C\sqrt{\nu}h\|\mathbf{w}\|_2\|\|\mathbf{v}\|\|_{\mathcal{B}},$$
 (4.13b)

$$|l_3(\mathbf{w}, \mathbf{v})| \le Ch \|\mathbf{w}\|_2 \|\|\mathbf{v}\|\|_{\mathcal{R}},$$
 (4.13c)

where C is a generic positive constant independent of v and h and may vary in each case.

Proof It follows from (4.2) and (4.5b) that

$$|l_{1}(\mathbf{w}, \mathbf{v})| = |\nu \mathbf{a}(\Pi_{h} \mathbf{w} - \mathbf{w}, \mathbf{v})|$$

$$\leq \nu \kappa_{2} \|\Pi_{h} \mathbf{w} - \mathbf{w}\|_{\mathcal{E}} \|\mathbf{v}\|_{\mathcal{E}}$$

$$\leq C \nu h \|\mathbf{w}\|_{2} \|\mathbf{v}\|_{\mathcal{E}}$$

$$\leq C \sqrt{\nu} h \|\mathbf{w}\|_{2} \|\mathbf{v}\|_{\mathcal{R}}.$$

On the other hand, the Cauchy–Schwarz inequality and (4.7) lead to

$$|l_{2}(\mathbf{w}, \mathbf{v})| = |\nu(\Delta \mathbf{w}, \mathcal{R}\mathbf{v} - \mathbf{v})_{\mathcal{T}_{h}}|$$

$$\leq \nu \|\mathbf{w}\|_{2} \|\mathcal{R}\mathbf{v} - \mathbf{v}\|_{0}$$

$$\leq C\nu h \|\mathbf{w}\|_{2} \|\mathbf{v}\|_{\mathcal{E}}$$

$$\leq C\sqrt{\nu}h \|\mathbf{w}\|_{2} \|\mathbf{v}\|_{\mathcal{R}}.$$

Using the Cauchy–Schwarz inequality, (4.7), (4.5c), (4.5a), and (4.8), we get the following upper bounds,

$$|l_{3}(\mathbf{w}, \mathbf{v})| = \left| (\mathcal{R}\Pi_{h}\mathbf{w} - \mathbf{w}, \mathcal{R}\mathbf{v})_{\mathcal{T}_{h}} \right|$$

$$\leq \left| (\mathcal{R}\Pi_{h}\mathbf{w} - \Pi_{h}\mathbf{w}, \mathcal{R}\mathbf{v})_{\mathcal{T}_{h}} \right| + \left| (\Pi_{h}\mathbf{w} - \mathbf{w}, \mathcal{R}\mathbf{v})_{\mathcal{T}_{h}} \right|$$

$$\leq Ch \|\Pi_{h}\mathbf{w}\|_{\mathcal{E}} \|\mathcal{R}\mathbf{v}\|_{0} + \|\Pi_{h}\mathbf{w} - \mathbf{w}\|_{0} \|\mathcal{R}\mathbf{v}\|_{0}$$

$$\leq Ch \|\mathbf{w}\|_{1} \|\|\mathbf{v}\|_{\mathcal{R}}.$$



In addition, we expand the continuity of $\mathbf{b}(\cdot, \cdot)$ in [22] to be relevant to the error equations (4.12) because $\mathbf{\chi}_h = \mathbf{u} - \Pi_h \mathbf{u} \notin \mathbf{V}_h$ and $\xi_h = p - \mathcal{P}_0 p \notin Q_h$.

Lemma 7 For any $\mathbf{v} \in \mathbf{V}_h$ and $q \in Q_h$, we have

$$|\mathbf{b}(\mathbf{v}, \xi_h)| \le Ch \|p\|_1 \|\mathbf{v}\|_{\mathcal{E}},\tag{4.14a}$$

$$|\mathbf{b}(\mathbf{\chi}_h, q)| \le Ch \|q\|_0 \|\mathbf{u}\|_2,$$
 (4.14b)

where C is a generic positive constant independent of v and h and may vary in each case.

Proof First, we use the Cauchy–Schwarz inequality to get

$$\begin{aligned} |\mathbf{b}(\mathbf{v}, \xi_h)| &= |(\nabla \cdot \mathbf{v}, \xi_h)_{\mathcal{T}_h} - \langle [\mathbf{v}] \cdot \mathbf{n}_e, \{\xi_h\} \rangle_{\mathcal{E}_h}| \\ &\leq C \left(\|\nabla \mathbf{v}\|_{0, \mathcal{T}_h} \|\xi_h\|_0 + \|h_e^{-1/2} [\mathbf{v}]\|_{0, \mathcal{E}_h} \|h_e^{1/2} \{\xi_h\}\|_{0, \mathcal{E}_h} \right). \end{aligned}$$

Then, the trace term is bounded by using the trace inequality (2.1) and interpolation error estimate (4.6),

$$\|h_e^{1/2}\{\xi_h\}\|_{0,\mathcal{E}_h}^2 \le C\left(\|\xi_h\|_0^2 + h^2\|\nabla \xi_h\|_{0,\mathcal{T}_h}^2\right) \le Ch^2\|p\|_1^2$$

because $\nabla \xi_h = \nabla (p - \mathcal{P}_0 p) = \nabla p$. Hence, the definition of the discrete H^1 -norm and estimate (4.6) imply

$$|\mathbf{b}(\mathbf{v}, \xi_h)| \leq Ch \|p\|_1 \|\mathbf{v}\|_{\mathcal{E}}.$$

Similarly, it follows from the Cauchy–Schwarz inequality, trace inequality (2.1), and (4.5b) that

$$\begin{split} |\mathbf{b}(\pmb{\chi}_h,q)| &\leq C \left(\|\nabla \pmb{\chi}_h\|_{0,\mathcal{T}_h} \|q\|_0 + \|h_e^{-1/2}[\pmb{\chi}_h]\|_{0,\mathcal{E}_h} \|h_e^{1/2}\{q\}\|_{0,\mathcal{E}_h} \right) \\ &\leq C \|q\|_0 \|\pmb{\chi}_h\|_{\mathcal{E}} \leq C h \|q\|_0 \|\mathbf{u}\|_2. \end{split}$$

Therefore, we prove error estimates of the PR-EG method in Algorithm 2.

Theorem 2 Let $(\mathbf{u}, p) \in [H_0^1(\Omega) \cap H^2(\Omega)]^d \times [L_0^2(\Omega) \cap H^1(\Omega)]$ be the solution to (1.1a)–(1.1c), and $(\mathbf{u}_h, p_h) \in \mathbf{V}_h \times Q_h$ be the discrete solution from the PR-EG method. Then, we have the following pressure-robust error estimates

$$\|\Pi_h \mathbf{u} - \mathbf{u}_h\|_{\mathcal{R}} \le Ch(\sqrt{\nu} + 1)\|\mathbf{u}\|_2,$$

 $\|\mathcal{P}_0 p - p_h\|_0 \le Ch(\nu + \sqrt{\nu})\|\mathbf{u}\|_2 + Ch^2\|\mathbf{u}\|_2.$

Proof We start with the error equation (4.12a),

$$\mathbf{b}(\mathbf{v}, \epsilon_h) = \nu \mathbf{a}(\mathbf{e}_h, \mathbf{v}) + \tilde{\mathbf{c}}(\mathbf{e}_h, \mathbf{v}) - l_1(\mathbf{u}, \mathbf{v}) - l_2(\mathbf{u}, \mathbf{v}) - l_3(\mathbf{u}, \mathbf{v}).$$

Then, it follows from (4.10) and (4.13) that

$$\mathbf{b}(\mathbf{v}, \epsilon_h) \le C \left(\|\mathbf{e}_h\|_{\mathcal{R}} + \sqrt{\nu} h \|\mathbf{u}\|_2 + h \|\mathbf{u}\|_2 \right) \|\mathbf{v}\|_{\mathcal{R}}.$$

From the inf-sup condition (4.11) with (4.4), we obtain

$$\|\epsilon_h\|_0 < C(\sqrt{\nu} + h) \left(\|\mathbf{e}_h\|_{\mathcal{R}} + \sqrt{\nu}h\|\mathbf{u}\|_2 + h\|\mathbf{u}\|_2 \right).$$
 (4.15)

We also choose $\mathbf{v} = \mathbf{e}_h$ and $q = \epsilon_h$ in (4.12) and substitute (4.12b) into (4.12a) to get

$$v\mathbf{a}(\mathbf{e}_h, \mathbf{e}_h) + \tilde{\mathbf{c}}(\mathbf{e}_h, \mathbf{e}_h) = -\mathbf{b}(\boldsymbol{\chi}_h, \boldsymbol{\epsilon}_h) + l_1(\mathbf{u}, \mathbf{e}_h) + l_2(\mathbf{u}, \mathbf{e}_h) + l_3(\mathbf{u}, \mathbf{e}_h).$$



Here, it follows from (4.14b) that

$$|\mathbf{b}(\mathbf{\chi}_h, \epsilon_h)| \le Ch \|\mathbf{u}\|_2 \|\epsilon_h\|_0. \tag{4.16}$$

Therefore, from (4.9), (4.13), and (4.16), we have

$$\|\|\mathbf{e}_h\|_{\mathcal{R}}^2 \le C \left(h\|\mathbf{u}\|_2\|\epsilon_h\|_0 + \sqrt{\nu}h\|\mathbf{u}\|_2\|\|\mathbf{e}_h\|\|_{\mathcal{R}} + h\|\mathbf{u}\|_2\|\|\mathbf{e}_h\|\|_{\mathcal{R}}\right).$$

We also replace $\|\epsilon_h\|_0$ by its upper bound in (4.15) omitting high-order terms,

$$\|\|\mathbf{e}_h\|\|_{\mathcal{R}}^2 \le C \left(\sqrt{\nu}h\|\mathbf{u}\|_2\|\|\mathbf{e}_h\|\|_{\mathcal{R}} + h\|\mathbf{u}\|_2\|\|\mathbf{e}_h\|\|_{\mathcal{R}} + \nu h^2\|\mathbf{u}\|_2^2\right).$$

In this case, the Young's inequality gives

$$\sqrt{\nu}h\|\mathbf{u}\|_{2}\|\mathbf{e}_{h}\|_{\mathcal{R}} \leq \frac{\nu h^{2}}{2\alpha}\|\mathbf{u}\|_{2}^{2} + \frac{\alpha}{2}\|\mathbf{e}_{h}\|_{\mathcal{R}}^{2},$$

$$h\|\mathbf{u}\|_{2}\|\mathbf{e}_{h}\|_{\mathcal{R}} \leq \frac{h^{2}}{2\alpha}\|\mathbf{u}\|_{2}^{2} + \frac{\alpha}{2}\|\mathbf{e}_{h}\|_{\mathcal{R}}^{2}.$$

Therefore, it follows from choosing a proper α that

$$\|\|\mathbf{e}_h\|\|_{\mathcal{R}}^2 \le Ch^2(\nu+1)\|\mathbf{u}\|_2^2$$

which implies that

$$\|\|\mathbf{e}_h\|\|_{\mathcal{R}} \le Ch(\sqrt{\nu}+1)\|\mathbf{u}\|_2.$$

If we apply this estimate to (4.15), then we obtain

$$\|\epsilon_h\|_0 \le Ch(\nu + \sqrt{\nu})\|\mathbf{u}\|_2 + Ch^2\|\mathbf{u}\|_2.$$

Remark 4 We emphasize that the error bounds in Theorem 2 are pressure-robust and have no detrimental effect from small ν . With $\nu \to 0$, the PR-EG method's velocity errors decrease in the optimal order, and pressure errors do in the second order (superconvergence is expected). This result implies that the PR-EG method produces stable and accurate solutions to the Brinkman equations in the Darcy regime.

In addition, we prove total error estimates showing the optimal orders of convergence in velocity and pressure.

Theorem 3 Under the same assumption of Theorem 2, we have the following error estimates

$$\|\|\mathbf{u} - \mathbf{u}_h\|\|_{\mathcal{R}} \le Ch(\sqrt{\nu} + 1)\|\mathbf{u}\|_2,$$

 $\|p - p_h\|_0 \le Ch((\nu + \sqrt{\nu})\|\mathbf{u}\|_2 + \|p\|_1).$

Proof We recall $\chi_h = \mathbf{u} - \Pi_h \mathbf{u}$ and observe the energy norm,

$$\|\|\boldsymbol{\chi}_h\|\|_{\mathcal{R}}^2 = \nu \|\boldsymbol{\chi}_h\|_{\mathcal{E}}^2 + \|\mathcal{R}\boldsymbol{\chi}_h\|_0^2.$$

Then, it follows from the triangle inequality, Theorem 3.1 in [6], (4.7), (4.5c), and (4.5a) that

$$\|\mathcal{R}\boldsymbol{\chi}_h\|_0 \leq \|\mathcal{R}\boldsymbol{\chi}_h - \boldsymbol{\chi}_h\|_0 + \|\boldsymbol{\chi}_h\|_0$$

$$\leq \|\mathcal{R}\mathbf{u} - \mathbf{u}\|_0 + \|\mathcal{R}\boldsymbol{\Pi}_h\mathbf{u} - \boldsymbol{\Pi}_h\mathbf{u}\|_0 + \|\boldsymbol{\chi}_h\|_0$$

$$< Ch\|\mathbf{u}\|_1$$



Hence, since $\|\mathbf{\chi}_h\|_{\mathcal{E}} \leq Ch\|\mathbf{u}\|_2$ from (4.5b), the error bound is

$$\|\|\boldsymbol{\chi}_h\|\|_{\mathcal{R}} \leq Ch\left(\sqrt{\nu}+1\right)\|\mathbf{u}\|_2.$$

Furthermore, the pressure error estimate is readily proved by the triangle inequality and interpolation error estimate (4.6).

In conclusion, the proposed PR-EG method solves the Brinkman equations in both the Stokes and Darcy regimes, having the optimal order of convergence for both velocity and pressure.

4.3 Error Estimates for the ST-EG Method

For comparison, we present error estimates of the ST-EG method in Algorithm 1.

Theorem 4 Let $(\mathbf{u}, p) \in [H_0^1(\Omega) \cap H^2(\Omega)]^d \times [L_0^2(\Omega) \cap H^1(\Omega)]$ be the solution to (1.1a)— (1.1c), and $(\mathbf{u}_h, p_h) \in \mathbf{V}_h \times Q_h$ be the discrete solution from the ST-EG method. Then, we have the following error estimates

$$\|\|\Pi_{h}\mathbf{u} - \mathbf{u}_{h}\|\| \le C \left[(\sqrt{\nu} + 1)h\|\mathbf{u}\|_{2} + \left(h + \frac{h}{\sqrt{\nu + c_{1}h^{2}}}\right) \|p\|_{1} \right],$$

$$\|\mathcal{P}_{0}p - p_{h}\|_{0} \le C \left[(\nu + \sqrt{\nu})h\|\mathbf{u}\|_{2} + (\sqrt{\nu} + 1)h\|p\|_{1} \right].$$

Proof See Appendix A.

Remark 5 Theorem 4 explains that the errors converge in the first order with h under the condition $h < \sqrt{v}$ easily satisfied in the Stokes regime. However, the velocity error in the Darcy regime may not decrease with h due to the pressure term in the velocity error bound, that is, when $\nu \to 0$,

$$\frac{h}{\sqrt{v + c_1 h^2}} \|p\|_1 \to \frac{1}{\sqrt{c_1}} \|p\|_1.$$

We will also confirm these theoretical results through numerical experiments. For this reason, the ST-EG method in Algorithm 1 may not be effective in solving the Brinkman equations with small v, which highlights the need for the PR-EG method in Algorithm 2.

5 Numerical Experiments

This section shows numerical experiments validating our theoretical results with two- and three-dimensional examples. The numerical methods in this paper and their discrete solutions are denoted as follows:

- $(\mathbf{u}_h^{\mathrm{ST}}, p_h^{\mathrm{ST}})$: Solution by the ST-EG method in Algorithm 1. $(\mathbf{u}_h^{\mathrm{PR}}, p_h^{\mathrm{PR}})$: Solution by the PR-EG method in Algorithm 2.

While considering the scaled Brinkman equations (1.1) with the parameter ν , we recall the error estimates for the ST-EG method in Theorem 4,

$$\|\Pi_h \mathbf{u} - \mathbf{u}_h^{\text{ST}}\| \lesssim (\sqrt{\nu} + 1)h\|\mathbf{u}\|_2 + \left(h + \frac{h}{\sqrt{\nu + c_1 h^2}}\right)\|p\|_1,$$
 (5.1a)



$$\|\mathcal{P}_0 p - p_h^{\text{ST}}\|_0 \lesssim (\nu + \sqrt{\nu})h\|\mathbf{u}\|_2 + (\sqrt{\nu} + 1)h\|p\|_1,$$
 (5.1b)

and the error estimates for the PR-EG method from Theorem 2

$$\||\Pi_h \mathbf{u} - \mathbf{u}_h^{\mathrm{PR}}\||_{\mathcal{R}} \lesssim (\sqrt{\nu} + 1)h\|\mathbf{u}\|_2, \tag{5.2a}$$

$$\|\mathcal{P}_0 p - p_h^{PR}\|_0 \lesssim (\nu + \sqrt{\nu})h\|\mathbf{u}\|_2 + h^2\|\mathbf{u}\|_2.$$
 (5.2b)

We mainly check the error estimates (5.1) and (5.2) by showing various numerical experiments with ν and h. We also display the difference between the numerical solutions for ST-EG and PR-EG in the Darcy regime, which shows that the PR-EG method is needed to obtain stable and accurate velocity solutions. Moreover, we present permeability tests by applying both EG methods. The permeability tests enhance the motivation of using the PR-EG method for the case of extreme viscosity or permeability.

We implement the numerical experiments using the authors' MATLAB codes developed based on iFEM [4]. The penalty parameter is chosen as $\rho = 3$ for all the numerical experiments.

5.1 Two Dimensional Tests

Let the computational domain be $\Omega = (0, 1) \times (0, 1)$. The velocity field and pressure are chosen as

$$\mathbf{u} = \begin{pmatrix} 10x^2(x-1)^2y(y-1)(2y-1) \\ -10x(x-1)(2x-1)y^2(y-1)^2 \end{pmatrix}, \quad p = 10(2x-1)(2y-1).$$

Then, the body force f and the Dirichlet boundary condition are obtained from (1.1) using the exact solutions.

5.1.1 Robustness and Accuracy Test with $\nu > 0$

We compare the ST-EG and PR-EG methods to see robustness and check their accuracy based on the error estimates (5.1) and (5.2). First, we interpret the ST-EG method's velocity error estimate (5.1a) depending on the relation between coefficient ν and mesh size h. The first-order convergence of the energy norm with h is guaranteed when $\nu \gg h^2$, but it is hard to tell any order of convergence when $\nu < h^2$ due to the term $h/\sqrt{\nu + c_1 h^2}$. On the other hand, the velocity error estimate for the PR-EG method (5.2a) means the first-order convergence in h regardless of ν .

In Fig. 1, we check the discrete H^1 -error for the velocity scaled by v, $\sqrt{v} \|\mathbf{u} - \mathbf{u}_h\|_{\mathcal{E}}$. It is a common component of the energy norm $\|\|\mathbf{u}-\mathbf{u}_h\|\|$ and $\|\|\mathbf{u}-\mathbf{u}_h\|\|_{\mathcal{R}}.$ The ST-EG method tends to produce errors increasing with $\mathcal{O}(h^{-1/2})$ when $h > \sqrt{\nu}$, while the errors decrease with $\mathcal{O}(h^{3/2})$ when $h < \sqrt{\nu}$. This result supports the error estimates (5.1a) (superconvergence may happen because we solve the problem on structured meshes) and means that a tiny mesh size is required for accurate solutions with small ν . However, the PR-EG method's errors uniformly show the first-order convergence, $\mathcal{O}(h)$, regardless of ν . This result supports the error estimates (5.2a), so the PR-EG method guarantees stable and accurate solutions in both the Stokes and Darcy regimes.

We fix $\nu = 10^{-6}$ and compare the velocity errors and solutions of the ST-EG and PR-EG methods. Table 1 displays the energy errors and their major components, the discrete H^1 errors scaled by ν and L^2 -errors. For the ST-EG method, the energy errors decrease in the half-order convergence because the L^2 -errors are dominant and decrease in the same order.



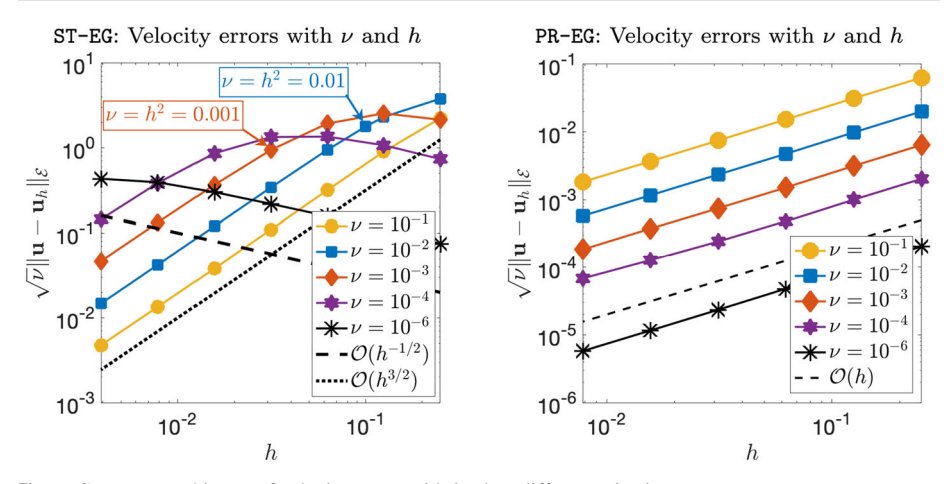


Fig. 1 Convergence history of velocity errors with h when different ν is given

Table 1 A mesh refinement study for the velocity errors of ST-EG and PR-EG with h when $\nu = 10^{-6}$

h	ST-EG							
	$\ \mathbf{u} - \mathbf{u}_h^{\text{ST}}\ $	Order	$\sqrt{v}\ \mathbf{u}-\mathbf{u}_h^{\mathrm{ST}}\ _{\mathcal{E}}$	Order	$\ \mathbf{u} - \mathbf{u}_h^{\text{ST}}\ _0$	Order		
1/4	2.926e+0	_	7.457e-2	_	2.925e+0	_		
1/8	2.120e+0	0.47	1.117e-1	-0.58	2.117e+0	0.47		
1/16	1.476e+0	0.52	1.572e-1	-0.49	1.467e+0	0.53		
1/32	1.037e+0	0.51	2.188e-1	-0.48	1.014e+0	0.53		
1/64	7.576e-1	0.45	3.010e-1	-0.46	6.952e - 1	0.55		
h	PR-EG							
	$\ \mathbf{u} - \mathbf{u}_h^{\mathtt{PR}}\ _{\mathcal{R}}$	Order	$\sqrt{ u}\ \mathbf{u}-\mathbf{u}_h^{\mathtt{PR}}\ _{\mathcal{E}}$	Order	$\ \mathbf{u} - \mathbf{u}_h^{\mathtt{PR}}\ _0$	Order		
1/4	1.265e-2	_	2.608e-4	_	1.265e-2	_		
1/8	2.493e-3	2.34	1.072e-4	1.28	2.491e-3	2.34		
1/16	5.267e-4	2.24	4.894e-5	1.13	5.244e-4	2.25		
1/32	1.209e-4	2.12	2.364e-5	1.05	1.186e-4	2.14		
1/64	3.035e-5	1.99	1.164e-5	1.02	2.803e-5	2.08		

However, the H^1 -errors keep increasing because $h \not < \sqrt{\nu} = 10^{-3}$, so the H^1 -errors will become dominant and deteriorate the order of convergence of the energy errors. On the other hand, using the PR-EG method, we expect from (5.2a) that the energy errors and major components converge in at least the first order of h. Indeed, Table 1 shows that the H^1 -errors decrease in the first order with h, while the L^2 -errors reduce in the second order. Since the energy error involve both H^1 - and L^2 -errors, the energy errors decrease in the second order because of the dominant L^2 -errors but eventually converge in the first order coming from the H^1 -errors.

In Fig. 2, the PR-EG method produces accurate velocity solutions clearly showing a vortex flow pattern when $\nu=10^{-6}$ and h=1/64. In contrast, the numerical velocity from the ST-EG method includes significant oscillations around the boundary of the domain.



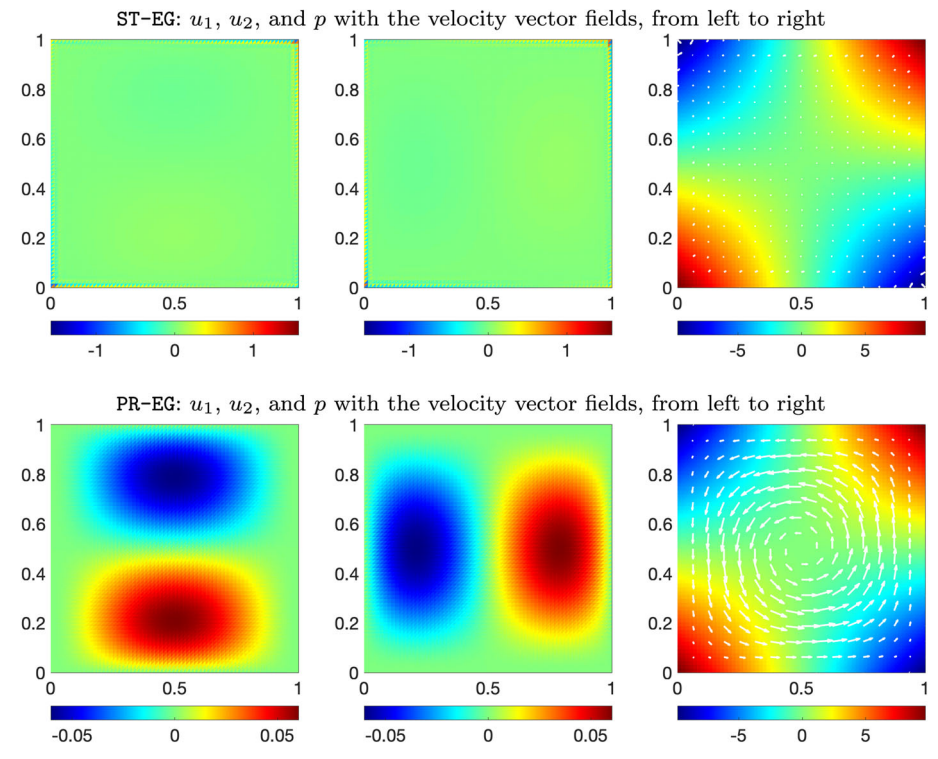


Fig. 2 Numerical solutions of ST-EG and PR-EG when $\nu=10^{-6}$ and h=1/64

Table 2 A mesh refinement study for the pressure errors of ST-EG and PR-EG with h when $v = 10^{-\overline{6}}$

h	ST-EG							
	$\ \mathcal{P}_0 p - p_h^{\text{ST}}\ _0$	Order	$\ p-p_h^{\rm ST}\ _0$	Order				
1/4	9.664e-1	_	1.358e+0	_				
1/8	4.273e-1	1.18	6.428e - 1	1.08				
1/16	2.125e-1	1.01	3.209e - 1	1.00				
1/32	1.109e - 1	0.94	1.636e - 1	0.97				
1/64	5.864e-2	0.92	8.399e-2	0.96				
h	PR-EG							
	$\ \mathcal{P}_0 p - p_h^{\mathtt{PR}}\ _0$	Order	$\ p-p_h^{\mathtt{PR}}\ _0$	Order				
1/4	3.899e-4	_	9.547e-1	_				
1/8	6.010e - 5	2.70	4.802e - 1	0.99				
1/16	7.703e-6	2.96	2.404e - 1	1.00				
1/32								
1/32	$8.865e{-7}$	3.12	1.203e - 1	1.00				



h	ST-EG						
	$\ \mathbf{u} - \mathbf{u}_h^{\mathtt{ST}}\ _{\mathcal{E}}$	Order	$\ \mathbf{u} - \mathbf{u}_h^{\text{ST}}\ _0$	Order	$\ \mathcal{P}_0 p - p_h^{\text{ST}}\ _0$	Order	
1/4	7.244e+0	_	2.940e-1	_	5.550e-2	-	
1/8	1.217e+1	-0.75	2.316e-1	0.34	2.369e-2	1.23	
1/16	1.785e+1	-0.55	1.659e-1	0.48	1.030e-2	1.20	
1/32	2.523e+1	-0.50	1.165e-1	0.51	5.077e-3	1.02	
1/64	3.548e+1	-0.49	8.174e-2	0.51	2.540e - 3	1.00	
h	PR-EG						
	$\ \mathbf{u} - \mathbf{u}_h^{\mathtt{PR}}\ _{\mathcal{E}}$	Order	$\ \mathbf{u} - \mathbf{u}_h^{\mathtt{PR}}\ _0$	Order	$\ \mathcal{P}_0 p - p_h^{\mathtt{PR}}\ _0$	Order	
1/4	1.735e+0	_	8.896e-2	-	1.724e-2	-	
1/8	6.491e-1	1.42	1.696e - 2	2.39	4.817e-3	1.84	
1/16	2.866e-1	1.18	3.693e - 3	2.20	1.220e-3	1.98	
1/32	1.371e-1	1.06	8.671e-4	2.09	$3.048e{-4}$	2.00	
1/64	6.750e - 2	1.02	2.107e-4	2.04	7.607e-5	2.00	

Table 3 A mesh refinement study for the velocity and pressure errors of the ST-EG and PR-EG with h when $\nu = 0$

Moreover, the pressure error estimates (5.1b) and (5.2b) tell us that the convergence order for the pressure errors is at least $\mathcal{O}(h)$ in both methods. However, the PR-EG method can produce superconvergent pressure errors because the term $h^2 \| p \|_1$ is dominant when ν is small. In Table 2, the pressure errors of the PR-EG method, $\| \mathcal{P}_0 p - p_h^{\text{PR}} \|_0$, decrease in at least $\mathcal{O}(h^2)$, which means superconvergence compared to the interpolation error estimate (4.6). On the other hand, the ST-EG method still yields pressure errors converging in the first order with h. Since the interpolation error is dominant in the total pressure errors $\| p - p_h \|_0$, the errors in Table 2 have the first-order convergence with h in both methods. Therefore, the numerical results support the pressure error estimates (5.1b) and (5.2b).

5.1.2 Performance in Darcy Regime ($\nu = 0$)

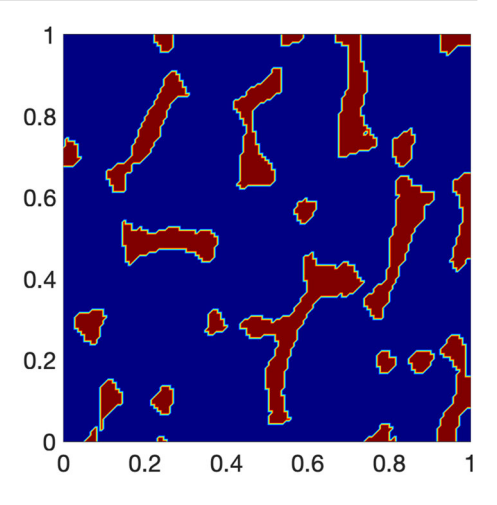
We numerically solve the Brinkman equations with $\nu=0$ (equivalent to Darcy flow) using the ST-EG and PR-EG methods. We consider the same domain $\Omega=(0,1)\times(0,1)$ and choose different velocity field and pressure

$$\mathbf{u} = \begin{pmatrix} \sin(\pi x)\sin(\pi y) \\ \cos(\pi x)\cos(\pi y) \end{pmatrix}, \quad p = \sin(\pi x)\cos(\pi y),$$

with a non-homogeneous Dirichlet boundary condition. In Table 3, the ST-EG method's velocity errors do not converge in the optimal convergence orders, while its pressure errors decrease in the first-order convergence, as expected in (5.1b). Some velocity errors are even increasing. From (5.1a), we can expect that the velocity errors will never converge in the optimal convergence order because it never holds $h < \sqrt{\nu}$. However, the PR-EG method guarantees the optimal convergence orders presented in (5.2a). The PR-EG method's pressure errors decrease in the second-order convergence as expected in (5.2b) with $\nu = 0$. This result demonstrates that the PR-EG method performs well with Darcy flow, producing stable and accurate velocity solutions and implying superconvergence of pressure errors.



Fig. 3 Permeability map; blue regions mean K = 1 and red regions mean $K = 10^{-6}$



5.1.3 Application to a Heterogeneous Porous Medium

In this test, we consider the original Brinkman equations

$$-\mu \Delta \mathbf{u} + \frac{\mu}{K} \mathbf{u} + \nabla p = \mathbf{f} \quad \text{in } \Omega, \tag{5.3a}$$

$$\nabla \cdot \mathbf{u} = 0 \quad \text{in } \Omega, \tag{5.3b}$$

with viscosity $\mu = 10^{-6}$ and permeability K given as the permeability map in Fig. 3.

The permeability map indicates that fluid tends to flow following the blue regions, so the magnitude of numerical velocity will be more significant in the blue regions than in the red ones. The blue and red regions imply:

- Blue regions: $\mu = 10^{-6}$ and K = 1 in (5.3a) $\Rightarrow \nu = 1$ in (1.1a) with scaled pressure and body force.
- Red regions: $\mu = K = 10^{-6}$ in (5.3a) $\Rightarrow \nu = 10^{-6}$ in (1.1a).

We set the velocity on the boundary of the domain as $\mathbf{u} = \langle 1, 0 \rangle$ and body force as $\mathbf{f} = \langle 1, 1 \rangle$. We mainly compare the magnitude of the numerical velocity obtained from the two methods in Fig. 4. We clearly see that the PR-EG method's velocity is more stable than the ST-EG method's velocity containing nonnegligible noises (or oscillations) around the boundary. This result tells that the PR-EG method is necessary for stable and accurate velocity solutions to the Brinkman equations with extreme viscosity and permeability.

5.2 Three Dimensional Tests

We consider a three-dimensional flow in a unit cube $\Omega = (0,1)^3$. The velocity field and pressure are chosen as

$$\mathbf{u} = \begin{pmatrix} \sin(\pi x)\cos(\pi y) - \sin(\pi x)\cos(\pi z) \\ \sin(\pi y)\cos(\pi z) - \sin(\pi y)\cos(\pi x) \\ \sin(\pi z)\cos(\pi x) - \sin(\pi z)\cos(\pi y) \end{pmatrix}, \quad p = \sin(\pi x)\sin(\pi y)\sin(\pi z).$$

The body force f and the Dirichlet boundary condition are given in the same manner as the two-dimensional example.



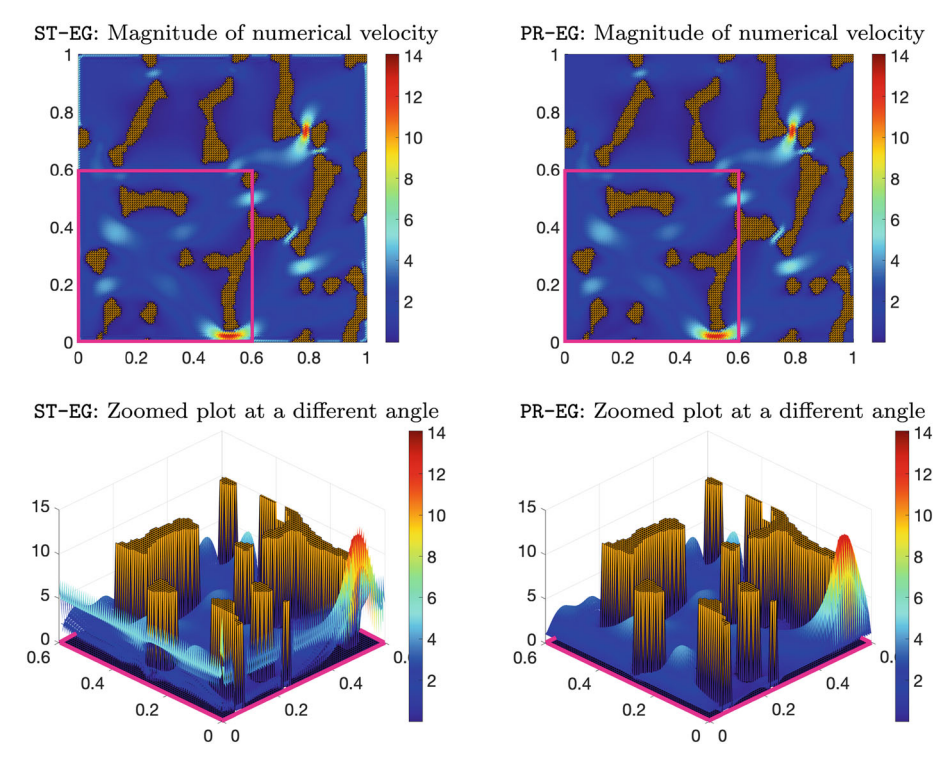


Fig. 4 Numerical velocity solutions of ST-EG and PR-EG on the permeability map

5.2.1 Robustness and Accuracy Test

In the two-dimensional tests, we checked that the condition $h < \sqrt{\nu}$ was required to guarantee the optimal order of convergence for the ST-EG method, while the PR-EG method showed a uniform performance in convergence independent of ν . We obtained the same result as in Fig. 1 from this three-dimensional test.

Table 4 displays the velocity solutions' energy errors and influential components, comparing the PR-EG method with ST-EG when $\nu=10^{-6}$. The ST-EG method's energy errors tend to decrease because the dominant L^2 -errors decrease, but the H^1 -errors scaled by ν increase. These H^1 -errors may make the energy errors nondecreasing until $h<\sqrt{\nu}=10^{-3}$. However, the PR-EG method guarantees at least first-order convergence for all the velocity errors, showing much smaller errors than the ST-EG method. This numerical result supports the velocity error estimates in (5.1a) and (5.2a), and we expect more accurate solutions from the PR-EG method when ν is small.

In addition, we compare numerical velocity solutions of the ST-EG and PR-EG methods when $\nu=10^{-6}$ and h=1/16 in Fig. 5. The velocity solutions of both methods seem to capture a three-dimensional vortex flow expected from the exact velocity. However, the velocity of the ST-EG method contains noises around the right-top and left-bottom corners, where the streamlines do not form a circular motion.

In Table 5, as expected in (5.1b), the ST-EG method's pressure errors decrease in at least first-order. On the other hand, the PR-EG method's pressure errors, $\|\mathcal{P}_0 p - p_h^{\text{UR}}\|_0$, decrease much faster, showing superconvergence. This phenomenon is expected by the pressure esti-



		•	•				
h	ST-EG						
	$\ \mathbf{u} - \mathbf{u}_h^{\mathtt{ST}}\ $	Order	$\sqrt{ u}\ \mathbf{u}-\mathbf{u}_h^{\mathtt{ST}}\ _{\mathcal{E}}$	Order	$\ \mathbf{u} - \mathbf{u}_h^{\text{ST}}\ _0$	Order	
1/4	1.086e+1	_	3.669e-1	_	1.085e+1	_	
1/8	8.553e+0	0.35	5.814e-1	-0.66	8.533e+0	0.35	
1/16	6.202e+0	0.46	$8.389e{-1}$	-0.53	6.145e+0	0.47	
1/32	4.418e+0	0.49	1.165e+0	-0.47	4.262e+0	0.53	
h	PR-EG						
	$\ \mathbf{u} - \mathbf{u}_h^{\mathtt{PR}}\ _{\mathcal{R}}$	Order	$\sqrt{v}\ \mathbf{u} - \mathbf{u}_h^{\mathtt{PR}}\ _{\mathcal{E}}$	Order	$\ \mathbf{u} - \mathbf{u}_h^{\mathtt{PR}}\ _0$	Order	
1/4	3.738e-1	-	2.684e-3	_	1.828e-1	-	
1/8	8.797e - 2	2.09	1.346e - 3	1.00	3.026e-2	2.59	
1/16	2.079e-2	2.08	6.600e - 4	1.03	6.203e - 3	2.29	
1/32	5.101e-3	2.03	3.256e-4	1.02	1.441e-3	2.11	

Table 4 A mesh refinement study for the velocity errors of the ST-EG and PR-EG with h when $\nu = 10^{-6}$

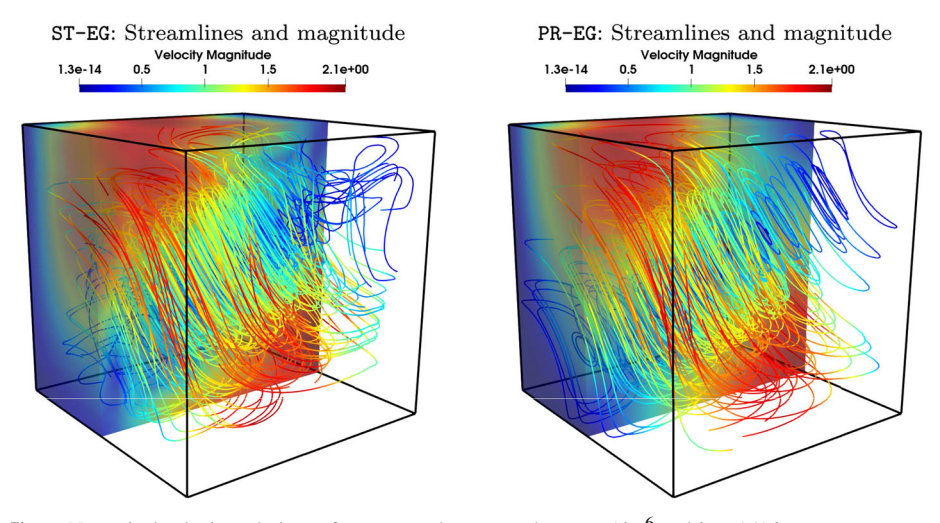


Fig. 5 Numerical velocity solutions of ST-EG and PR-EG when $\nu=10^{-6}$ and h=1/16

mate (5.2b) when ν is small. Moreover, the orders of convergence of the total pressure errors, $||p-p_h||_0$, for both methods are approximately one due to the interpolation error.

5.2.2 Application to Different Permeability Regions

We apply piecewise constant permeability to the original Brinkman equations (5.3) in the cube domain $\Omega = (0, 1)^3$,

$$K(\mathbf{x}) = \begin{cases} 10^{-6} & \text{if } |\mathbf{x}| \le (0.25)^2, \\ 1 & \text{otherwise.} \end{cases}$$

The other conditions are given as; viscosity $\mu = 10^{-6}$, boundary condition $\mathbf{u} = \langle 1, 0, 0 \rangle$, and body force $\mathbf{f} = \langle 1, 1, 1 \rangle$.



Table 5 A mesh refinement study for the pressure errors of the ST-EG and PR-EG with h when $\nu=10^{-6}$

h	ST-EG							
	$\ \mathcal{P}_0 p - p_h^{\text{ST}}\ _0$	Order	$\ p-p_h^{\rm ST}\ _0$	Order				
1/4	1.564e+0	_	3.357e+0	_				
1/8	5.599e-1	1.48	1.613e+0	1.06				
1/16	1.781e-1	1.65	7.804e - 1	1.05				
1/32	5.717e-2	1.64	$3.846e{-1}$	1.02				
h	PR-EG							
	$\ \mathcal{P}_0 p - p_h^{\mathrm{PR}}\ _0$	Order	$\ p-p_h^{\mathtt{PR}}\ _0$	Order				
1/4	1.109e-1	_	2.973e+0	_				
1/8	1.241e-2	3.16	1.513e+0	0.98				
1/16	1.344e - 3	3.21	7.598e - 1	0.99				
1/32	1.609e-4	3.06	3.804e - 1	1.00				

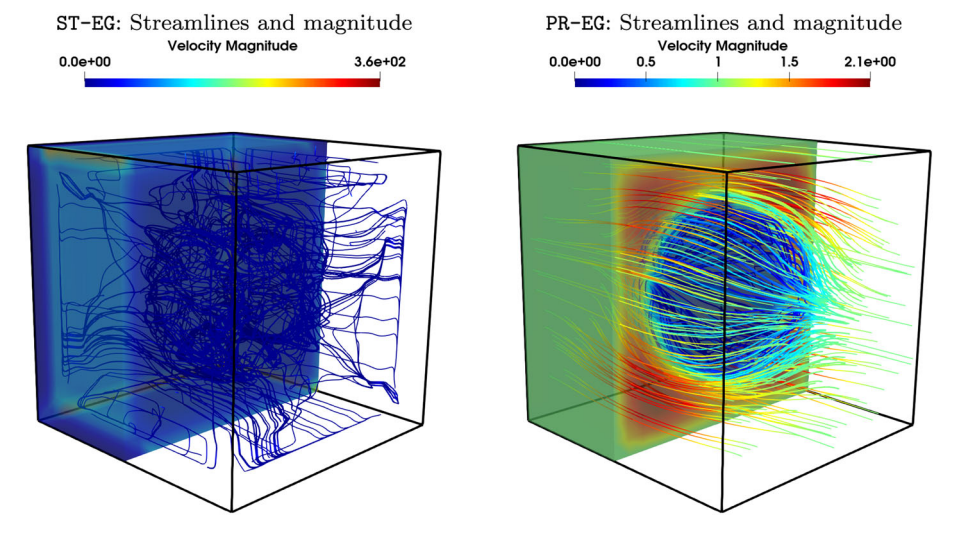


Fig. 6 Numerical velocity solutions of ST-EG and PR-EG when h=1/16

We expect the fluid flow to be faster out of the ball with large permeability, and it tends to avoid the ball and be affected by the boundary velocity. The streamlines and colored magnitude of the PR-EG method's velocity in Fig. 6 exactly show such an expectation on the fluid flow, while the ST-EG method fails to provide a reliable velocity solution.

6 Conclusion

In this paper, we proposed a pressure-robust numerical method for the Brinkman equations with minimal degrees of freedom based on the EG piecewise linear velocity and constant pressure spaces [22]. To derive the robust method, we used the velocity reconstruction operator [12] mapping the EG velocity to the first-order Brezzi–Douglas–Marini space. Then, we replaced the EG velocity in the Darcy term and the test function on the right-hand side



with the reconstructed velocity. With this simple modification, the robust EG method showed uniform performance in both the Stokes and Darcy regimes compared to the standard EG method requiring the mesh restriction $h < \sqrt{\nu}$ that is impractical in the Darcy regime. We also validated the error estimates and performance of the standard and robust EG methods through several numerical tests with two- and three-dimensional examples.

Our efficient and robust EG method for the Brinkman equations can be extended to various Stokes-Darcy modeling problems, such as coupled models with an interface and timedependent models. Also, the proposed EG method can be extended for nonlinear models, such as nonlinear Brinkman models for non-Newtonian fluid and unsteady Brinkman-Forchheimer models.

Funding Lin Mu's work was supported in part by the U.S. National Science Foundation grant DMS-2309557.

Data Availability The datasets generated during and/or analyzed during the current study are available from the corresponding author upon reasonable request.

Declarations

Conflict of interest The authors have not disclosed any Conflict of interest.

Appendix A: Proof of Theorem 4

We recall the error functions

$$\chi_h := \mathbf{u} - \Pi_h \mathbf{u}, \quad \mathbf{e}_h := \Pi_h \mathbf{u} - \mathbf{u}_h, \quad \xi_h := p - \mathcal{P}_0 p, \quad \epsilon_h := \mathcal{P}_0 p - p_h$$

and derive error equations.

Lemma 8 For any $\mathbf{v} \in \mathbf{V}_h$ and $q \in Q_h$, we have

$$\nu \mathbf{a}(\mathbf{e}_h, \mathbf{v}) + \mathbf{c}(\mathbf{e}_h, \mathbf{v}) - \mathbf{b}(\mathbf{v}, \epsilon_h) = l_1(\mathbf{u}, \mathbf{v}) + l_4(\mathbf{u}, \mathbf{v}) + \mathbf{b}(\mathbf{v}, \xi_h),$$

$$\mathbf{b}(\mathbf{e}_h, q) = -\mathbf{b}(\mathbf{y}_h, q),$$

where $l_1(\mathbf{u}, \mathbf{v})$ is defined in Lemma 5, and the other supplement bilinear form is defined as follows:

$$l_4(\mathbf{u},\mathbf{v}) := (\Pi_h \mathbf{u} - \mathbf{u},\mathbf{v})_{\mathcal{T}_h}$$

Proof We have $-(\Delta \mathbf{u}, \mathbf{v})_{\mathcal{T}_h} = \mathbf{a}(\mathbf{u}, \mathbf{v})$ for any $\mathbf{v} \in \mathbf{V}_h$ from [22], which implies that

$$-\nu(\Delta \mathbf{u}, \mathbf{v})_{\mathcal{T}_h} = \nu \mathbf{a}(\Pi_h \mathbf{u}, \mathbf{v}) - \nu \mathbf{a}(\Pi_h \mathbf{u} - \mathbf{u}, \mathbf{v}).$$

The definition of $\mathbf{c}(\cdot, \cdot)$ also gives

$$(\mathbf{u}, \mathbf{v})_{\mathcal{T}_h} = \mathbf{c}(\Pi_h \mathbf{u}, \mathbf{v}) - (\Pi_h \mathbf{u} - \mathbf{u}, \mathbf{v})_{\mathcal{T}_h},$$

and integration by parts and continuity of p lead to

$$(\nabla p, \mathbf{v})_{T_h} = \sum_{T \in T} \langle p, \mathbf{v} \cdot \mathbf{n}_T \rangle_{\partial T} - (p, \nabla \cdot \mathbf{v})_T = -\mathbf{b}(\mathbf{v}, p).$$

Thus, the equation (1.1a) imposes

$$v\mathbf{a}(\Pi_h\mathbf{u},\mathbf{v}) + \mathbf{c}(\Pi_h\mathbf{u},\mathbf{v}) - \mathbf{b}(\mathbf{v},p) = (\mathbf{f},\mathbf{v}) + l_1(\mathbf{u},\mathbf{v}) + l_4(\mathbf{u},\mathbf{v}).$$



By comparing this equation with (3.1a) in the ST-EG method, we arrive at

$$v\mathbf{a}(\mathbf{e}_h, \mathbf{v}) + \mathbf{c}(\mathbf{e}_h, \mathbf{v}) - \mathbf{b}(\mathbf{v}, \epsilon_h) = l_1(\mathbf{u}, \mathbf{v}) + l_4(\mathbf{u}, \mathbf{v}) + \mathbf{b}(\mathbf{v}, \xi_h).$$

Moreover, it follows from the continuity of \mathbf{u} and (3.1b) that

$$(\nabla \cdot \mathbf{u}, q)_{\mathcal{T}_h} = \mathbf{b}(\mathbf{u}, q) = 0 = \mathbf{b}(\mathbf{u}_h, q),$$

which implies the second equation.

In what follows, we prove an estimate for the supplemental bilinear form in Lemma 8.

Lemma 9 Assume that $\mathbf{w} \in [H^2(\Omega)]^d$ and $\mathbf{v} \in \mathbf{V}_h$. Then, we have

$$|l_4(\mathbf{w}, \mathbf{v})| \le Ch^2 ||\mathbf{w}||_2 |||\mathbf{v}||$$

where C is a generic positive constant independent of v and h.

Proof Using the Cauchy–Schwarz inequality and (4.5a), we get the following upper bounds

$$|l_4(\mathbf{w}, \mathbf{v})| = |(\Pi_h \mathbf{w} - \mathbf{w}, \mathbf{v})_{\mathcal{T}_h}|$$

$$\leq ||\Pi_h \mathbf{w} - \mathbf{w}||_0 ||\mathbf{v}||_0$$

$$< Ch^2 |\mathbf{w}|_2 ||\mathbf{v}||.$$

Proof of Theorem 4

Proof We apply (4.10), (4.8), (4.14a), (4.13), (4.3), and Lemma 9 to the first error equation in Lemma 8.

$$\mathbf{b}(\mathbf{v}, \epsilon_h) = \nu \mathbf{a}(\mathbf{e}_h, \mathbf{v}) + \mathbf{c}(\mathbf{e}_h, \mathbf{v}) - l_1(\mathbf{u}, \mathbf{v}) - l_4(\mathbf{u}, \mathbf{v}) - \mathbf{b}(\mathbf{v}, \xi_h)$$

$$\leq C \left(\|\mathbf{e}_h\| + \sqrt{\nu} h \|\mathbf{u}\|_2 + h^2 \|\mathbf{u}\|_2 + \frac{h}{\sqrt{\nu + c_1 h^2}} \|p\|_1 \right) \|\mathbf{v}\|.$$

Thus, the results in Lemma 4 with (4.4) imply

$$\|\epsilon_h\|_0 \le C(\sqrt{\nu} + h) \left(\|\|\mathbf{e}_h\|\| + \sqrt{\nu}h\|\mathbf{u}\|_2 + h^2\|\mathbf{u}\|_2 + \frac{h}{\sqrt{\nu + c_1h^2}}\|p\|_1 \right).$$

We choose $\mathbf{v} = \mathbf{e}_h$ and $q = \epsilon_h$ and substitute $\mathbf{b}(\mathbf{e}_h, \epsilon_h)$ with $-\mathbf{b}(\mathbf{\chi}_h, \epsilon_h)$ to obtain

$$v\mathbf{a}(\mathbf{e}_h, \mathbf{e}_h) + \mathbf{c}(\mathbf{e}_h, \mathbf{e}_h) = -\mathbf{b}(\boldsymbol{\chi}_h, \boldsymbol{\epsilon}_h) + l_1(\mathbf{u}, \mathbf{e}_h) + l_4(\mathbf{u}, \mathbf{e}_h) + \mathbf{b}(\mathbf{e}_h, \boldsymbol{\xi}_h).$$

In this case, we estimate the term $\mathbf{b}(\boldsymbol{\chi}_h, \epsilon_h)$ using (4.14b),

$$|\mathbf{b}(\mathbf{\chi}_h, \epsilon_h)| \leq Ch \|\mathbf{u}\|_2 \|\epsilon_h\|_0.$$

The term $\mathbf{b}(\mathbf{e}_h, \xi_h)$ is estimated by using (4.14a) and (4.3),

$$|\mathbf{b}(\mathbf{e}_h, \xi_h)| \le Ch \|p\|_1 \|\mathbf{e}_h\|_{\mathcal{E}} \le C \frac{h}{\sqrt{\nu + c_1 h^2}} \|p\|_1 \|\mathbf{e}_h\|.$$

Hence, it follows from (4.9), (4.13), Lemma 9, and the above results that



$$\|\|\mathbf{e}_h\|\|^2 \le C \left(h \|\mathbf{u}\|_2 \|\epsilon_h\|_0 + \sqrt{\nu} h \|\mathbf{u}\|_2 \|\|\mathbf{e}_h\|\| + h^2 \|\mathbf{u}\|_2 \|\|\mathbf{e}_h\|\| + \frac{h}{\sqrt{\nu + c_1 h^2}} \|p\|_1 \|\|\mathbf{e}_h\|\| \right).$$

Then, by using the bound of $\|\epsilon_h\|_0$ and omitting high-order terms $(h^3 \text{ or } h^4)$, we obtain an upper bound

$$h\|\mathbf{u}\|_{2}\|\epsilon_{h}\|_{0} \leq C\left((\sqrt{\nu}+h)h\|\mathbf{u}\|_{2}\|\|\mathbf{e}_{h}\|\|+\nu h^{2}\|\mathbf{u}\|_{2}^{2}+h^{2}\|\|\mathbf{u}\|_{2}\|p\|_{1}\right)$$

because $\sqrt{\nu} + h \le (\sqrt{2/c_1})\sqrt{\nu + c_1h^2}$. If we apply the Young's inequality to each term with a positive constant α , we have

$$\begin{split} & \sqrt{\nu}h\|\mathbf{u}\|_{2}\|\mathbf{e}_{h}\| \leq \frac{\nu h^{2}}{2\alpha}\|\mathbf{u}\|_{2}^{2} + \frac{\alpha}{2}\|\mathbf{e}_{h}\|^{2}, \\ & h^{2}\|\mathbf{u}\|_{2}\|\mathbf{e}_{h}\| \leq \frac{h^{4}}{2\alpha}\|\mathbf{u}\|_{2}^{2} + \frac{\alpha}{2}\|\mathbf{e}_{h}\|^{2}, \\ & h^{2}\|\mathbf{u}\|_{2}\|p\|_{1} \leq \frac{h^{2}}{2\alpha}\|\mathbf{u}\|_{2}^{2} + \frac{\alpha h^{2}}{2}\|p\|_{1}^{2}, \\ & \frac{h}{\sqrt{\nu + c_{1}h^{2}}}\|p\|_{1}\|\|\mathbf{e}_{h}\| \leq \frac{h^{2}}{2\alpha(\nu + c_{1}h^{2})}\|p\|_{1}^{2} + \frac{\alpha}{2}\|\|\mathbf{e}_{h}\|\|^{2}. \end{split}$$

Therefore, a proper α implies

$$\|\|\mathbf{e}_h\|\|^2 \le C \left[(\nu+1)h^2 \|\mathbf{u}\|_2^2 + \left(h^2 + \frac{h^2}{\nu + c_1 h^2}\right) \|p\|_1^2 \right],$$

so we finally get

$$\|\|\mathbf{e}_h\|\| \le C \left[(\sqrt{\nu} + 1)h \|\mathbf{u}\|_2 + \left(h + \frac{h}{\sqrt{\nu + c_1 h^2}} \right) \|p\|_1 \right].$$

On the other hand, we observe intermediate estimates and omit high-order terms (h^2 or h^3). so we show the pressure error estimate,

$$\|\epsilon_h\|_0 \le C \left[(\sqrt{\nu} + h) \|\|\mathbf{e}_h\|\| + \nu h \|\mathbf{u}\|_2 + h \|p\|_1 \right].$$

Thus, we bound $\|\mathbf{e}_h\|$ with the velocity error estimate, so we finally obtain

$$\|\epsilon_h\|_0 \le C \left[(\nu + \sqrt{\nu})h \|\mathbf{u}\|_2 + (\sqrt{\nu} + 1)h \|p\|_1 \right],$$

when omitting h^2 -terms.

References

- 1. Anaya, V., Gatica, G.N., Mora, D., Ruiz-Baier, R.: An augmented velocity-vorticity-pressure formulation for the Brinkman equations. Int. J. Numer. Meth. Fluids 79(3), 109-137 (2015)
- 2. Burman, E.: Pressure projection stabilizations for Galerkin approximations of Stokes' and Darcy's problem. Numer. Methods Partial Differ. Equ.: Int. J. 24(1), 127–143 (2008)
- Burman, E., Hansbo, P.: Stabilized Crouzeix-Raviart element for the Darcy-Stokes problem. Numer. Methods Partial Differ. Equ.: Int. J. 21(5), 986–997 (2005)



- Chen, L.: iFEM: An Integrated Finite Element Methods Package in MATLAB. Technical Report, University of California at Irvine (2009)
- Correa, M.R., Loula, A.F.D.: A unified mixed formulation naturally coupling Stokes and Darcy flows. Comput. Methods Appl. Mech. Eng. 198(33–36), 2710–2722 (2009)
- Durán, R.: Mixed finite element methods. Mixed finite elements, compatibility conditions, and applications pp. 1–44 (2008)
- Fu, G., Jin, Y., Qiu, W.: Parameter-free superconvergent H(div)-conforming HDG methods for the Brinkman equations. IMA J. Numer. Anal. 39(2), 957–982 (2019)
- 8. Führer, T., Videman, J.: First-order system least-squares finite element method for singularly perturbed Darcy equations. ESAIM: Math. Model. Numer. Anal. **57**(4), 2283–2300 (2023)
- Gatica, G.N., Gatica, L.F., Sequeira, F.A.: Analysis of an augmented pseudostress-based mixed formulation for a nonlinear Brinkman model of porous media flow. Comput. Methods Appl. Mech. Eng. 289, 104–130 (2015)
- Hannukainen, A., Juntunen, M., Stenberg, R.: Computations with finite element methods for the Brinkman problem. Comput. Geosci. 15, 155–166 (2011)
- Howell, J.S., Neilan, M., Walkington, N.J.: A dual-mixed finite element method for the Brinkman problem. SMAI J. Comput. Math. 2, 1–17 (2016)
- Hu, X., Lee, S., Mu, L., Yi, S.Y.: Pressure-robust enriched Galerkin methods for the Stokes equations. J. Comput. Appl. Math. 436, 115449 (2024)
- Jia, J., Lee, Y.J., Feng, Y., Wang, Z., Zhao, Z.: Hybridized weak Galerkin finite element methods for Brinkman equations. Electron. Res. Arch. 29(3), 2489–2516 (2021)
- Johnny, G., Neilan, M.: A family of nonconforming elements for the Brinkman problem. IMA J. Numer. Anal. 32(4), 1484–1508 (2012)
- Könnö, J., Stenberg, R.: Non-conforming finite element method for the Brinkman problem. In: Numerical Mathematics and Advanced Applications 2009: Proceedings of ENUMATH 2009, the 8th European Conference on Numerical Mathematics and Advanced Applications, Uppsala, July 2009, pp. 515–522. Springer (2010)
- Könnö, J., Stenberg, R.: Numerical computations with H(div)-finite elements for the Brinkman problem. Comput. Geosci. 16, 139–158 (2012)
- Linke, A.: A divergence-free velocity reconstruction for incompressible flows. C.R. Math. 350(17–18), 837–840 (2012)
- Mardal, K.A., Tai, X.C., Winther, R.: A robust finite element method for Darcy–Stokes flow. SIAM J. Numer. Anal. 40(5), 1605–1631 (2002)
- Mu, L.: A uniformly robust H(div) weak Galerkin finite element methods for Brinkman problems. SIAM J. Numer. Anal. 58(3), 1422–1439 (2020)
- Vassilevski, P.S., Villa, U.: A mixed formulation for the Brinkman problem. SIAM J. Numer. Anal. 52(1), 258–281 (2014)
- Xie, X., Xu, J., Xue, G.: Uniformly-stable finite element methods for Darcy–Stokes–Brinkman models. J. Comput. Math., pp. 437–455 (2008)
- Yi, S.Y., Hu, X., Lee, S., Adler, J.H.: An enriched Galerkin method for the Stokes equations. Comput. Math. Appl. 120, 115–131 (2022)
- Yi, S.Y., Lee, S., Zikatanov, L.T.: Locking-free enriched Galerkin method for linear elasticity. SIAM J. Numer. Anal. 60(1), 52–75 (2022)
- Zhao, L., Chung, E.T., Lam, M.F.: A new staggered DG method for the Brinkman problem robust in the Darcy and Stokes limits. Comput. Methods Appl. Mech. Eng. 364, 112986 (2020)

Publisher's Note Springer Nature remains neutral with regard to jurisdictional claims in published maps and institutional affiliations.

Springer Nature or its licensor (e.g. a society or other partner) holds exclusive rights to this article under a publishing agreement with the author(s) or other rightsholder(s); author self-archiving of the accepted manuscript version of this article is solely governed by the terms of such publishing agreement and applicable law.

